Isocurvature Perturbation of Weakly Interacting Massive Particles and Small Scale Structure

Ki-Young Choi,[1,*] Jinn-Ouk Gong,[2,3,†] and Chang Sub Shin[4,‡]
[1]Korea Astronomy and Space Science Institute, Daejeon 305-348, Korea
[2]Asia Pacific Center for Theoretical Physics, Pohang 790-784, Korea
[3]Department of Physics, Postech, Pohang 790-784, Korea
[4]Department of Physics and Astronomy, Rutgers University, Piscataway, New Jersey 08854, USA
(Received 20 July 2015; revised manuscript received 5 October 2015; published 17 November 2015)

The adiabatic perturbation of dark matter is damped during the kinetic decoupling due to the collision with a relativistic component on subhorizon scales. However, the isocurvature part is free from damping and could be large enough to make a substantial contribution to the formation of small scale structure. We explicitly study the weakly interacting massive particles as dark matter with an early matter dominated period before radiation domination and show that the isocurvature perturbation is generated during the phase transition and leaves an imprint in the observable signatures for small scale structure.

DOI: 10.1103/PhysRevLett.115.211302 PACS numbers: 95.35.+d, 14.80.Ly, 98.80.Cq

Introduction.—The formation of large scale structure is consistent with nonrelativistic dark matter (DM) independent of its nature. Small scale structure, however, depends on the microphysics of DM and the corresponding evolution in the early Universe [1–4]. For weakly interacting massive particles (WIMPs), the kinetic decoupling is a crucial stage to determine the size of the smallest object [5,6]: during the process of kinetic decoupling collisional damping smears out the inhomogeneities below the corresponding damping scale. After kinetic decoupling, WIMPs can move freely and this leads to additional damping below the free streaming scale. For neutralino DM, the kinetic decoupling scale is set when the temperature is 10 MeV–1 GeV for the mass between 100 GeV and TeV [7].

In the radiation dominated era (RD), while the "adiabatic" component of DM perturbation on subhorizon scales experiences oscillations followed by collisional damping [8], the isocurvature perturbation between DM and radiation,

$$S \equiv 3H\left(\frac{\delta\rho_m}{\dot{\rho}_m} - \frac{\delta\rho_r}{\dot{\rho}_r}\right) = \delta_m - \frac{3}{4}\delta_r, \tag{1}$$

remains constant without damped oscillations [9,10]. This property was used to explain large scale structure with baryon isocurvature perturbation [9], which is ruled out now by the adiabatic constraint from the cosmic microwave background (CMB) [11]. However, large isocurvature perturbation on small scales is not constrained by the CMB observations and can give observable signatures in small scale structure.

In this Letter, we show how large isocurvature perturbation of WIMPs can be generated for scales that enter the horizon before the kinetic decoupling. If $S = 0$ at the onset of RD, it remains so during kinetic equilibrium. Instead, if an early matter dominated era precedes RD, a sizable amount of S can be generated. We note that this isocurvature perturbation will not be damped even if the kinetic decoupling happens after the transition to RD.

Dark matter in nonthermal background.—In the early Universe, it happens often that the energy density of the Universe is dominated by a nonrelativistic matter that subsequently decays into relativistic particles. This nonrelativistic matter includes a coherently oscillating scalar field like an inflaton, or massive fields which decay very late, such as curvaton, moduli, and so on. As an illustration, we consider this dominating nonrelativistic matter as a scalar ϕ with a decay rate Γ_ϕ. Accordingly, we call the epoch during which ϕ dominates the energy density the scalar dominated era (SD). In the background there are three species of fluid: ϕ, radiation, and DM. Their evolutions are governed by the continuity equations,

$$\dot{\rho}_\phi + 3H\rho_\phi = -\Gamma_\phi\rho_\phi, \tag{2}$$

$$\dot{\rho}_r + 4H\rho_r = (1-f_m)\Gamma_\phi\rho_\phi + \frac{\langle\sigma_a v\rangle}{M}[\rho_m^2 - (\rho_m^{\rm eq})^2], \tag{3}$$

$$\dot{\rho}_m + 3H\rho_m = f_m\Gamma_\phi\rho_\phi - \frac{\langle\sigma_a v\rangle}{M}[\rho_m^2 - (\rho_m^{\rm eq})^2], \tag{4}$$

where M is the mass of the DM particle, f_m is the fraction of the decay of ϕ into DM, $\langle\sigma_a v\rangle$ is the thermal averaged annihilation cross section of DM and $\rho_m^{\rm eq} \approx M^4(2\pi M/T)^{-3/2}\exp(-M/T)$ is the energy density of DM in thermal equilibrium. Here, radiation is the relativistic particles thermalized quickly when produced from the decay of ϕ, and thus the temperature T is properly defined by its energy density $\rho_r = \pi^2 g_* T^4/30$ with g_* being the effective degrees of freedom of the relativistic particles in thermal equilibrium. The reheating temperature is then approximately given by $T_{\rm reh} \approx (\pi^2 g_*/90)^{-1/4}\sqrt{m_{\rm Pl}\Gamma_\phi}$. For successful big bang nucleosynthesis, we require that $T_{\rm reh}$ must be larger than $\mathcal{O}(\mathrm{MeV})$ [12].

While radiation is produced directly from the decay of ϕ, DM can be produced in several different ways [13]. For simplicity, we assume that DM is produced only from radiation by scatterings and set $f_m = 0$. Even in this case, a sizable amount of DM can be produced from thermal plasma. If the interaction of DM with plasma is large enough, they could be in thermal equilibrium. WIMP is one such example, which is intimately coupled to the relativistic plasma and decoupled when $T/M \sim 1/20$, depending on the annihilation cross section $\langle\sigma_a v\rangle$ [14]. The freeze-out may happen during SD or RD after the scalar decay. For the latter case, there will be no difference from the thermal WIMP in the standard scenario. Therefore, in our study, we will focus on the case that WIMPs are decoupled during SD.

In Fig. 1, we show the evolution of the background energy densities of ϕ, radiation, and DM by solving Eqs. (2)–(4). During SD, ρ_r scales as $\rho_r \propto a^{-3/2}$ due to the continuous production from the scalar decay and thus the effective equation of state during SD is $-1/2$. DM is frozen during SD, and its energy density decreases simply proportional to a^{-3} afterward. However, the interactions by collisions continue until RD.

Evolution of perturbations.—Now we consider the evolution of perturbations. For this, we use the Newtonian gauge with the metric

$$ds^2 = -(1+2\Phi)dt^2 + a^2(1-2\Psi)\delta_{ij}dx^i dx^j. \quad (5)$$

The perturbation equations can be derived from the Boltzmann equation for each component ($\alpha = \phi$, r, and m) and they are given by [8,15]

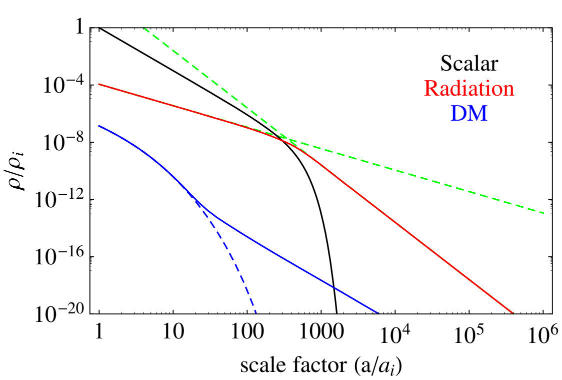

FIG. 1 (color online). The evolution of the energy densities of the scalar (black), radiation (red), and DM (blue), respectively, with respect to the initial total energy density. The blue dashed line is the equilibrium energy density of WIMP, and green dashed lines denote the asymptotic behavior of radiation energy density. DM freezes out at $a/a_i \simeq 20$ and RD starts from $a/a_i \simeq 300$.

$$\dot{\delta}_\alpha + (1+w_\alpha)\frac{\theta_\alpha}{a} - 3(1+w_\alpha)\dot{\Psi} = \frac{1}{\rho_\alpha}(\delta Q_\alpha - Q_\alpha\delta_\alpha + Q_\alpha\Phi), \quad (6)$$

$$\dot{\theta}_\alpha + (1-3w_\alpha)H\theta_\alpha + \frac{\Delta\Phi}{a} + \frac{w_\alpha}{1+w_\alpha}\frac{\Delta\delta_\alpha}{a} = \frac{1}{\rho_\alpha}\left[\frac{\partial_i Q^i_{(\alpha)}}{1+w_\alpha} - Q_\alpha\theta_\alpha\right], \quad (7)$$

where $\theta_\alpha \equiv \nabla\cdot v_\alpha = \partial_i v^i_\alpha$ is the velocity divergence field, $w_\phi = w_m = 0$, and $w_r = 1/3$. At leading order of T/M, the energy-momentum transfer functions Q_α and δQ_α can be calculated from the Boltzmann equation as

$$Q_\phi = -\Gamma_\phi\rho_\phi, \quad (8)$$

$$Q_r = \Gamma_\phi\rho_\phi + \frac{\langle\sigma_a v\rangle}{M}[\rho_m^2 - (\rho_m^{\rm eq})^2], \quad (9)$$

$$Q_m = -\frac{\langle\sigma_a v\rangle}{M}[\rho_m^2 - (\rho_m^{\rm eq})^2], \quad (10)$$

$$\delta Q_\phi = -\Gamma_\phi\rho_\phi\delta_\phi, \quad (11)$$

$$\delta Q_r = \Gamma_\phi\rho_\phi\delta_\phi + \frac{2\langle\sigma_a v\rangle}{M}\left[\rho_m^2\delta_m - (\rho_m^{\rm eq})^2\frac{M}{T}\frac{\delta_r}{4}\right], \quad (12)$$

$$\delta Q_m = -\frac{2\langle\sigma_a v\rangle}{M}\left[\rho_m^2\delta_m - (\rho_m^{\rm eq})^2\frac{M}{T}\frac{\delta_r}{4}\right], \quad (13)$$

and $\partial_i Q^i_{(\alpha)}$ by

$$\partial_i Q^i_{(\phi)} = -\Gamma_\phi\rho_\phi\theta_\phi, \quad (14)$$

$$\partial_i Q^i_{(r)} = \Gamma_\phi\rho_\phi\theta_\phi + \frac{\langle\sigma_a v\rangle}{M}\left[\rho_m^2\theta_m - \frac{4}{3}(\rho_m^{\rm eq})^2\frac{M}{2\pi T}^{1/2}\theta_r\right] - c_e\frac{\langle\sigma_e v\rangle}{M}\rho_m\rho_r(\theta_r - \theta_m), \quad (15)$$

$$\partial_i Q^i_{(m)} = -\frac{\langle\sigma_a v\rangle}{M}\left[\rho_m^2\theta_m - \frac{4}{3}(\rho_m^{\rm eq})^2\frac{M}{2\pi T}^{1/2}\theta_r\right] + c_e\frac{\langle\sigma_e v\rangle}{M}\rho_m\rho_r(\theta_r - \theta_m), \quad (16)$$

where we have put $f_m = 0$. In the above equations, we have included the elastic scattering cross section between radiation and DM σ_e which keeps DM and radiation in kinetic equilibrium until they decouple at $T_{\rm kd}$ set by $c_e\langle\sigma_e v\rangle\rho_r/M|_{T=T_{\rm kd}} = H(T_{\rm kd})$, with $c_e = \mathcal{O}(1)$ being dependent on the model due to the different momentum dependence of σ_e.

The 00 component of the perturbed Einstein equation governs the evolution of the metric perturbations,

$$\frac{\Delta}{a^2}\Psi - 3H(\dot{\Psi} + H\Phi) = \frac{1}{2m_{\rm Pl}^2}(\rho_\phi\delta_\phi + \rho_r\delta_r + \rho_m\delta_m). \tag{17}$$

In the absence of the anisotropic tensor, we can set $\Phi = \Psi$, which then closes the above set of equations. This is possible since ϕ and radiation, which dominate the energy density, are isotropic in our setup. Note that the effects of the anisotropic shear and nonvanishing sound speed of DM, $c_s \sim \sqrt{T/M}$, can be important after kinetic decoupling for scales smaller than the free streaming length $k_{\rm fr}^{-1}$. In Ref. [16], it is shown that when the free streaming length is much shorter than the scale $k_{\rm kd}^{-1}$ that enters the horizon at the moment of kinetic decoupling, we can take an approximation that solving the Boltzmann equations first in the perfect fluid limit while maintaining the elastic scattering, and then multiplying the solution by the Gaussian suppression term. Actually, this limit is also physically interesting, because two different damping scales can be more clearly distinguished.

In this Letter, we consider the hierarchies among scales as $k_{\rm fr}^{-1} < k_{\rm reh}^{-1} < k_{\rm kd}^{-1}$, where $k_{\rm reh}^{-1}$ is the scale that enters the horizon at $T = T_{\rm reh}$. This means that the free streaming scale enters the horizon during SD and that kinetic decoupling occurs during RD. The large hierarchy between $k_{\rm fr}^{-1}$ and $k_{\rm kd}^{-1}$ can be obtained when M is big enough while the elastic scattering is mediated by a field much lighter than DM. In this case, the freeze-out abundance also could be large, but the subsequent dilution by entropy injection from the scalar decay can provide the correct amount of the present DM density [17,18]. For WIMP, we find [19]

$$k_{\rm kd}^{-1} = 0.86\frac{10~{\rm MeV}}{T_{\rm kd}}\left(\frac{g_{*s}}{10.75}\right)^{1/3}\left(\frac{10.75}{g_*}\right)^{1/2}~{\rm pc}, \tag{18}$$

$$k_{\rm reh}^{-1} = k_{\rm kd}^{-1}\frac{T_{\rm kd}}{T_{\rm reh}}, \tag{19}$$

$$k_{\rm fr}^{-1} = \int_{t_{\rm kd}}^{t_0}\frac{dt}{a}c_s \approx k_{\rm kd}^{-1}\sqrt{\frac{T_{\rm kd}}{M}}\log\left(\frac{T_{\rm kd}}{T_{\rm eq}}\right), \tag{20}$$

where g_{*s} is the effective number of light species for entropy and $T_{\rm eq} = \mathcal{O}({\rm eV})$ is the temperature at matter-radiation equality.

In Fig. 2, we show the evolution of perturbations on three different scales. During SD, the perturbations are adiabatic on super-horizon scales since both radiation and DM are produced from a single source ϕ, which set the initial values of perturbations as $\delta_\phi(a_i) = 2\delta_r(a_i) = -2\Phi_i$ and $\delta_m(a_i) \approx M\delta_r(a_i)/(4T_i)$, with T_i being determined from $\rho_r(a_i)$. During the transition from SD to RD, Φ rescales from Φ_i to $10\Phi_i/9$ on superhorizon scales and accordingly δ_r changes from $-\Phi_i$ to $-2(10/9)\Phi_i$. Meanwhile, at early times when DM is in thermal (chemical) equilibrium, $\delta_m \propto a^{3/8}$ and is reduced to $-5\Phi_i/3$ during RD which follows the adiabatic condition $\delta_m = 3\delta_r/4$.

While for modes which enter the horizon after kinetic decoupling ($k_{\rm kd}^{-1} < k^{-1}$), δ_r oscillates and δ_m grows logarithmically as shown in the left panel of Fig. 2, for the modes which enter before kinetic decoupling ($k_{\rm reh}^{-1} < k^{-1} < k_{\rm kd}^{-1}$) δ_m oscillates together with δ_r and is damped, which is known as collisional damping. The nonvanishing subhorizon entropy perturbation appears due to the damping of δ_m as shown in the middle panel of Fig. 2.

An interesting feature happens for the modes that enter the horizon during SD but after the free streaming scale enters ($k_{\rm fr}^{-1} < k^{-1} < k_{\rm reh}^{-1}$) as in the right panel of Fig. 2. During the transition from SD to RD, δ_m does *not* follow δ_r, and the isocurvature perturbation is generated. In this period, DM is no longer produced after chemical freeze-out and the number density is frozen while radiation is still being produced from ϕ. The continuous entropy injection becomes the source of the isocurvature perturbation between DM and radiation. This perturbation still persists even after kinetic decoupling. Before calculating its analytic expression we explicitly show why it is not damped from the solution for δ_m during RD [16],

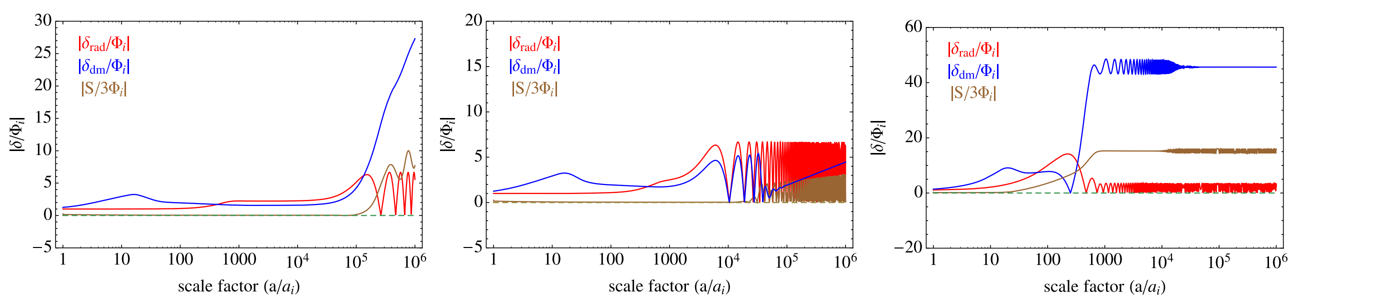

FIG. 2 (color online). The evolution of the density contrast of the radiation (red), DM (blue), and the isocurvature perturbation (brown) with respect to the initial gravitational potential for $k_{\rm kd}^{-1} < k^{-1}$ ($k = 0.1k_{\rm kd}$, left), $k_{\rm reh}^{-1} < k^{-1} < k_{\rm kd}^{-1}$ ($k = 5k_{\rm kd} = 0.5k_{\rm reh}$, middle), and $k_{\rm fr}^{-1} < k^{-1} < k_{\rm reh}^{-1}$ ($k = 50k_{\rm kd} = 5k_{\rm reh} = 0.8k_{\rm fr}$, right). We have set $M = 5$ TeV, $T_{\rm reh} = 0.1$ GeV, and $T_{\rm kd} = 0.01$ GeV.

$$\delta_m = \Delta_k\left[\left(\frac{k}{\sqrt{3}aH}\right)^{-2}\cos\left(\frac{k}{\sqrt{3}aH}+\phi_k\right) - \left(\frac{k}{\sqrt{3}aH}\right)^{-3}\left(1-\frac{k^2}{3a^2H^2}\right)\sin\left(\frac{k}{\sqrt{3}aH}+\phi_k\right) + \int_{k/(\sqrt{3}aH)}^{\infty}\frac{\cos(x+\phi_k)}{x}dx\right] + A_k(t)\log\left(\frac{k}{\sqrt{3}aH}\right) + B_k(t), \tag{21}$$

where Δ_k and ϕ_k are k-dependent constants while $A_k(t)$ and $B_k(t)$ vary in time. Their time dependence is determined by the elastic scattering term as

$$\dot{A}_k + c_e\frac{\langle\sigma_e v\rangle\rho_r}{aM}A_k = 9c_e\frac{\langle\sigma_e v\rangle\rho_r}{aM}\left[\cos\left(\frac{k}{\sqrt{3}aH}+\phi_k\right) + \frac{k}{2\sqrt{3}aH}\sin\left(\frac{k}{\sqrt{3}aH}+\phi_k\right)\right],$$
$$\dot{B}_k + \dot{A}_k\log\left(\frac{k}{\sqrt{3}aH}\right) = 0. \tag{22}$$

The values of Δ_k, ϕ_k, $A_k(t_{\rm reh})$, and $B_k(t_{\rm reh})$ are given at the onset of RD, and for adiabatic modes they are

$$\Delta_k = -10\Phi_i, \qquad \phi_k = 0, \qquad A_k(t_{\rm reh}) = -10\Phi_i,$$
$$B_k^{\rm ad}(t_{\rm reh}) = -10\Phi_i\left(\gamma_E - \frac{1}{2}\right), \tag{23}$$

where $\gamma_E \approx 0.577$ is the Euler-Mascheroni constant. Then on superhorizon scales $k \ll aH$ we can recover $-5\Phi_i/3$ during RD. For the modes which enters during RD ($k_{\rm reh}^{-1} < k^{-1}$), the solution is [16]

$$A_k, B_k^{\rm ad} \propto \exp\left[-0.8\left(\frac{k}{2\sqrt{3}k_{\rm kd}}\right)^{[(4+n)/(5+n)]}\right] \tag{24}$$

for $\langle\sigma_e v\rangle \propto T^{2+n}$, which clearly shows the damping for $k^{-1} \ll k_{\rm kd}^{-1}$ due to the collision with radiation.

Here it is important to note that in Eq. (22) only $\dot{B}_k$ appears. The additional constant term to the adiabatic one is not damped away even in the kinetic equilibrium and decoupling periods. As a result, for $k^{-1} \ll k_{\rm kd}^{-1}$, δ_m is dominated by the isocurvature perturbation: $B_k = B_k^{\rm iso} + B_k^{\rm ad} \simeq B_k^{\rm iso}$.

Generation of isocurvature perturbation.—For the modes that enter the horizon during SD after chemical decoupling of DM, δ_ϕ grows linearly,

$$\delta_\phi(a) = -2\Phi_i - \frac{2}{3}\Phi_i\left[\frac{k}{a_iH(a_i)}\right]^2\frac{a}{a_i}, \tag{25}$$

and then logarithmically during RD. Meanwhile, δ_r grows during SD, since radiation is continuously produced from the decay of ϕ. However, after the transition from SD to RD, this enhancement is lost and δ_r oscillates with heavily suppressed amplitude [1].

During kinetic equilibrium, DM is tightly coupled to radiation, so that $\theta_m \approx \theta_r$. Ignoring the effect of DM annihilation, the relevant equations for δ_m and δ_r are, from Eq. (6),

$$\dot{\delta}_m \approx -\frac{\theta_r}{a}, \tag{26}$$

$$\dot{\delta}_r \approx -\frac{4}{3}\frac{\theta_r}{a} + \frac{\Gamma_\phi\rho_\phi}{\rho_r}(\delta_\phi - \delta_r), \tag{27}$$

where we have neglected $\mathcal{O}(1)$ contribution. From SD to the transition period, both δ_r and Φ are subdominant compared to δ_ϕ, and $\rho_r \approx 2\Gamma_\phi\rho_\phi/5H$. Then the isocurvature perturbation is

$$S(t_{\rm reh}) \approx -\frac{3}{4}\int_{t_i}^{t_{\rm reh}} dt\frac{\Gamma_\phi\rho_\phi\delta_\phi}{\rho_r} \approx \frac{5}{4}\Phi_i\left(\frac{k}{k_{\rm reh}}\right)^2. \tag{28}$$

As can be read from Eq. (26), unlike δ_m, δ_r is sourced by both θ_r and δ_ϕ because there is steady production of radiation from ϕ. The corresponding isocurvature part becomes $B_k^{\rm iso}$.

While the isocurvature perturbation can avoid the damping due to the collision, the diffusion by the free streaming still exists. Considering the damping effect due to free streaming, as discussed before we may add a Gaussian suppression factor to δ_m as

$$\delta_m \approx \exp\left(-\frac{k^2}{2k_{\rm fr}^2}\right)\frac{5}{4}\Phi_i\left(\frac{k}{k_{\rm reh}}\right)^2, \tag{29}$$

where the free streaming scale $k_{\rm fr}^{-1}$ is estimated as (19). Based on these results, it is straightforward to calculate the

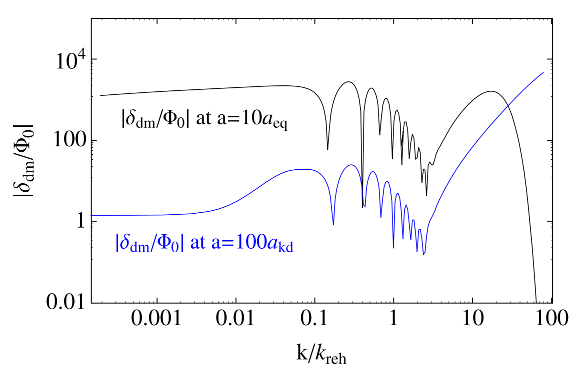

FIG. 3 (color online). Density contrast of DM with $M = 5$ TeV, $T_{\rm reh} = 0.1$ GeV, and $T_{\rm kd} = 0.01$ GeV.

evolution of perturbation during the subsequent matter dominated era, the transfer function, and the mass function. In Fig. 3, we show δ_m at later stages at $a = 100a_{\rm kd}$ and $10a_{\rm eq}$.

Implications.—At the heart of our finding is that despite the damping of the conventional adiabatic perturbation of DM due to a large elastic scattering rate between DM and the standard model particles, the DM isocurvature perturbation survives the collisional damping until kinetic decoupling. This unsuppressed perturbation on a small scale can give rise to a large number of DM clumps, such as compact mini haloes [20,21].

Since DM can annihilate efficiently in the clumps, these haloes can serve as the sources of highly luminous gamma rays which can be well observed with the ongoing or future gamma-ray telescope like the Fermi-LAT [22] or Cerenkov Telescope Array [23]. They can also be the sources of neutrinos [24], detectable by IceCube [25]. Furthermore, they can leave an imprint in the CMB by changing the reionization history of the Universe [26], produce a microlensing light curve [27,28], or change the direct detection rate [29].

The requisite for a large enough DM isocurvature perturbation is a sufficient hierarchy between DM freeze-out and reheating to have a long enough early MD. This is easily realized with a low reheating temperature, which happens ubiquitously in many theoretical models when the heavy particle dominates and decays in the early Universe. Those models include the neutralino DM in the low reheating temperature [30,31] and the scenario of decaying heavy particles such as moduli, gravitino [32], or axino [18]. Considering both astrophysical and cosmological observations and DM theories should give more information about the early history of the Universe before BBN and the properties of DM.

J. G. acknowledges the Max-Planck-Gesellschaft, the Korea Ministry of Education, Science and Technology, Gyeongsangbuk-Do and Pohang City for the support of the Independent Junior Research Group at the Asia Pacific Center for Theoretical Physics. J. G. is also supported by a Starting Grant through the Basic Science Research Program of the National Research Foundation of Korea (2013R1A1A1006701). C. S. S. is supported in part by DOE Grants No. DOE-SC0010008, No. DOE-ARRA-SC0003883, and No. DOE-DE-SC0007897.

[*]kiyoungchoi@kasi.re.kr
[†]jinn-ouk.gong@apctp.org
[‡]changsub@physics.rutgers.edu

[1] A. L. Erickcek and K. Sigurdson, Phys. Rev. D **84**, 083503 (2011).
[2] G. Barenboim and J. Rasero, J. High Energy Phys. 04 (2014) 138.
[3] J. J. Fan, O. Özsoy, and S. Watson, Phys. Rev. D **90**, 043536 (2014).
[4] A. Loeb and M. Zaldarriaga, Phys. Rev. D **71**, 103520 (2005).
[5] S. Hofmann, D. J. Schwarz, and H. Stöcker, Phys. Rev. D **64**, 083507 (2001).
[6] A. M. Green, S. Hofmann, and D. J. Schwarz, J. Cosmol. Astropart. Phys. 08 (2005) 003.
[7] T. Bringmann, New J. Phys. **11**, 105027 (2009).
[8] C. P. Ma and E. Bertschinger, Astrophys. J. **455**, 7 (1995).
[9] P. J. E. Peebles, Astrophys. J. **315**, L73 (1987).
[10] W. Hu and N. Sugiyama, Phys. Rev. D **51**, 2599 (1995).
[11] P. A. R. Ade *et al.* (Planck Collaboration), arXiv:1502.01589.
[12] S. Hannestad, Phys. Rev. D **70**, 043506 (2004).
[13] H. Baer, K. Y. Choi, J. E. Kim, and L. Roszkowski, Phys. Rep. **555**, 1 (2015).
[14] B. W. Lee and S. Weinberg, Phys. Rev. Lett. **39**, 165 (1977).
[15] S. Dodelson, *Modern Cosmology* (Academic Press, New York, NY, 2003).
[16] E. Bertschinger, Phys. Rev. D **74**, 063509 (2006).
[17] G. Arcadi and P. Ullio, Phys. Rev. D **84**, 043520 (2011).
[18] K. Y. Choi, J. E. Kim, H. M. Lee, and O. Seto, Phys. Rev. D **77**, 123501 (2008).
[19] E. W. Kolb and M. S. Turner, Front. Phys. **69**, 1 (1990).
[20] J. Diemand, B. Moore, and J. Stadel, Nature (London) **433**, 389 (2005).
[21] T. Bringmann, P. Scott, and Y. Akrami, Phys. Rev. D **85**, 125027 (2012).
[22] B. Bertoni, D. Hooper, and T. Linden, arXiv:1504.02087.
[23] J. Carr *et al.* (CTA Consortium Collaboration), arXiv:1508.06128.
[24] Y. Yang, G. Yang, and H. Zong, Phys. Rev. D **87**, 103525 (2013).
[25] M. G. Aartsen *et al.* (IceCube Collaboration), Phys. Rev. D **88**, 122001 (2013).
[26] V. S. Berezinsky, V. I. Dokuchaev, and Y. N. Eroshenko, Usp. Fiz. Nauk **184**, 3 (2014) [Phys. Usp. **57**, 1 (2014)].
[27] M. Ricotti and A. Gould, Astrophys. J. **707**, 979 (2009).
[28] F. Li, A. L. Erickcek, and N. M. Law, Phys. Rev. D **86**, 043519 (2012).
[29] M. Kamionkowski and S. M. Koushiappas, Phys. Rev. D **77**, 103509 (2008).
[30] G. B. Gelmini and P. Gondolo, Phys. Rev. D **74**, 023510 (2006).
[31] L. Roszkowski, S. Trojanowski, and K. Turzynski, J. High Energy Phys. 11 (2014) 146.
[32] K. Kohri, M. Yamaguchi, and J. Yokoyama, Phys. Rev. D **72**, 083510 (2005).